



The alcohol acetyltransferase Eat1 is located in yeast mitochondria

Kruis, A. J., Mars, A. E., Kengen, S. W. M., Borst, J. W., van der Oost, J., & Weusthuis, R. A.

This is a "Post-Print" accepted manuscript, which has been published in "Applied and Environmental Microbiology"

This version is distributed under a non-commercial no derivatives Creative Commons



([CC-BY-NC-ND](https://creativecommons.org/licenses/by-nc-nd/4.0/)) user license, which permits use, distribution, and reproduction in any medium, provided the original work is properly cited and not used for commercial purposes. Further, the restriction applies that if you remix, transform, or build upon the material, you may not distribute the modified material.

Please cite this publication as follows:

Kruis, A. J., Mars, A. E., Kengen, S. W. M., Borst, J. W., van der Oost, J., & Weusthuis, R. A. (2018). The alcohol acetyltransferase Eat1 is located in yeast mitochondria. *Applied and Environmental Microbiology*. DOI: 10.1128/AEM.01640-18

You can download the published version at:

<https://doi.org/10.1128/AEM.01640-18>

1 **The alcohol acetyltransferase Eat1 is located in yeast mitochondria**

2 Aleksander J. Kruis<sup>a,b</sup>, Astrid E. Mars<sup>c</sup>, Servé W. M. Kengen<sup>a</sup>, Jan Willem Borst<sup>d</sup>,  
3 John van der Oost<sup>a</sup>, Ruud A. Weusthuis<sup>b</sup>

4 Affiliations

5 a – Laboratory of Microbiology, Wageningen University and Research, Stippeneng 4, 6708  
6 WE Wageningen, The Netherlands

7 b – Bioprocess Engineering, Wageningen University and Research, Droevendaalsesteeg 1,  
8 6708 PB Wageningen, The Netherlands

9 c – Biobased Products, Wageningen University and Research, Bornse Weilanden 9, 6708  
10 WG Wageningen, The Netherlands

11 d – Laboratory of Biochemistry, Wageningen University & Research, Stippeneng 4, 6708 WE  
12 Wageningen, The Netherlands

13

## 14 **Abstract**

15 Eat1 is a recently discovered alcohol acetyltransferase responsible for bulk ethyl acetate  
16 production in yeasts such as *Wickerhamomyces anomalus* and *Kluyveromyces lactis*. These  
17 yeasts have the potential to become efficient biobased ethyl acetate producers. However,  
18 some fundamental features of Eat1 are still not understood, which hampers the rational  
19 engineering of efficient production strains. The cellular location of Eat1 in yeast is one of  
20 these features. To reveal its location, Eat1 was fused with yEGFP to allow intracellular  
21 tracking. Despite the current assumption that bulk ethyl acetate production occurs in the  
22 yeast cytosol, most of Eat1 localised to the mitochondria of *K. lactis* CBS 2359  $\Delta ku80$ . We  
23 then compared five bulk ethyl acetate-producing yeasts in iron-limited chemostats with  
24 glucose as carbon source. All yeasts produced ethyl acetate under these conditions. This  
25 strongly suggests that the mechanism and location of bulk ethyl acetate synthesis are similar  
26 in these yeast strains. Furthermore, an *in silico* analysis showed that Eat1 proteins from  
27 various yeasts were mostly predicted as mitochondrial. Altogether, it is concluded that Eat1-  
28 catalyzed ethyl acetate production occurs in yeast mitochondria. This study has added new  
29 insights to bulk ethyl acetate synthesis in yeast, which is relevant for developing efficient  
30 production strains.

## 31 **Importance**

32 Ethyl acetate is a common bulk chemical that is currently produced from petrochemical  
33 sources. Several Eat1-containing yeast strains naturally produce high amounts of ethyl  
34 acetate and are potential cell factories for the production of biobased ethyl acetate. Rational  
35 design of the underlying metabolic pathways may result in improved production strains, but it  
36 requires fundamental knowledge on the function of Eat1. A key feature is the location of Eat1  
37 in the yeast cell. The precursors for ethyl acetate synthesis can be produced in multiple  
38 cellular compartments through different metabolic pathways. The location of Eat1 determines  
39 the relevance of each pathway, which will provide future targets for the metabolic  
40 engineering of bulk ethyl acetate production in yeast.

## 41 Introduction

42 Ethyl acetate is a valuable bulk chemical and an important aroma compound in fermented  
43 foods (1). Industrially, ethyl acetate is produced from petrochemical resources, but biological  
44 production routes have been explored in recent years. Yeasts are prominent natural ethyl  
45 acetate producers. Ester production is well known in *Saccharomyces cerevisiae*, which  
46 typically produces between 8 and 32 mg/L ethyl acetate in beer fermentations (2). Several  
47 non-*Saccharomyces* yeast species produce ethyl acetate from carbohydrates at a much  
48 higher yield than *S. cerevisiae* (3). Ethyl acetate yields up to 51.4 % of the theoretical  
49 pathway maximum have been reported in *Kluyveromyces marxianus* (4). Other bulk ethyl  
50 acetate producing yeasts include *Wickerhamomyces anomalus* (5, 6), *Cyberlindnera fabianii*  
51 (7) and *Kluyveromyces lactis* (8).

52 Alcohol acetyl transferases (AATs) are the main ethyl acetate producing enzymes which use  
53 acetyl-CoA and ethanol as substrate. Most research on ethyl acetate producing AATs in  
54 yeast is based on Atf1 and Atf2 from *S. cerevisiae* (9, 10). A *S. cerevisiae* strain lacking *atf1*  
55 and *atf2* produced 50 % less ethyl acetate compared to the parental strain (11). Homologs of  
56 Atf1 and Atf2 are present in bulk ethyl acetate producing yeasts (12, 13).

57 The prevailing hypothesis on the physiological function of bulk ethyl acetate production  
58 suggests that it is produced as an overflow metabolite under conditions where the TCA cycle  
59 does not function optimally (3, 14). Yeasts that naturally produce bulk amounts of ethyl  
60 acetate are Crabtree-negative. They oxidise glucose and other carbohydrates to pyruvate in  
61 the cytosol. Under aerobic conditions, Crabtree-negative yeasts preferentially transport the  
62 pyruvate to the mitochondria. There, it is further oxidised via pyruvate dehydrogenase to  
63 acetyl-CoA (Figure 1, Reaction I) and subsequently oxidized in the TCA cycle (19). Ethyl  
64 acetate is formed under conditions where the efficiency of the TCA cycle is impaired by e.g.  
65 iron or oxygen limitation (15, 16). As a consequence, acetyl-CoA cannot enter the TCA cycle  
66 and accumulates in the mitochondria. It is assumed that yeasts use an AAT-catalysed

67 reaction to relieve the acetyl-CoA accumulation and regenerate free CoA (3, 18). Ethyl  
68 acetate is formed in the process. This hypothesis would imply that mitochondrial acetyl-CoA  
69 accumulation causes ethyl acetate production (17).

70 Ethanol is the second substrate needed for ethyl acetate synthesis by AATs. Crabtree-  
71 negative yeasts typically do not form ethanol under aerobic conditions. However,  
72 unfavourable conditions, such as iron limitation, lead to ethanol formation in *K. marxianus*  
73 even in the presence of oxygen (16, 20). Ethanol is produced from pyruvate via acetaldehyde  
74 in the cytosol (Figure 1). The acetaldehyde may also be converted to acetate and further to  
75 cytosolic acetyl-CoA via acetyl-CoA synthetase (Figure 1, Reaction II). This reaction is  
76 essential in most yeasts as it supplies acetyl-CoA for fatty acid synthesis (21). However,  
77 during aerobic growth on sugars, the acetyl-CoA flux in the cytosol is much lower compared  
78 to the mitochondria (22). It is therefore unlikely that it contributes significantly to bulk ethyl  
79 acetate synthesis. Moreover, bulk ethyl acetate synthesis in yeast does not occur in the  
80 absence of oxygen (17). Under anaerobic conditions, carbohydrate catabolism occurs in the  
81 cytosol, and mitochondrial acetyl-CoA cannot accumulate. These observations strongly  
82 suggest that acetyl-CoA used to synthesise ethyl acetate is derived from the mitochondria.

83 Atf1, Atf2 and their homologs appear to be cytosolic, or located in the endoplasmic reticulum  
84 (23–25). A translocation step would therefore be required to transfer acetyl-CoA from the  
85 mitochondria to the cytosol. Some yeasts are able to translocate acetyl-CoA to the cytosol in  
86 the form of citrate. This shunt relies on the presence of ATP-citrate lyase, which converts  
87 citrate to acetyl-CoA and oxaloacetate at the expense of one ATP (Figure 1, Reaction III).  
88 The reaction is typically present in oleaginous yeasts, such as *Yarrowia lipolytica* or  
89 *Rhodospiridium toruloides* (26, 27). It is not known if ATP-citrate lyase is present in any of  
90 the yeasts that produce high amounts of ethyl acetate. Without this enzyme, transport of  
91 acetyl-CoA from the mitochondria to the cytosol is unlikely.

92 The hypothetical function of bulk ethyl acetate production is the release of excess  
93 mitochondrial acetyl-CoA. However, the previously assumed ethyl acetate producing  
94 enzymes are located either in the cytosol or in the endoplasmic reticulum. These locations do  
95 not match with the mitochondrial function of ethyl acetate formation. Recently, a new family  
96 of AATs was discovered, designated Eat1. This family catalyses ethyl acetate synthesis in *S.*  
97 *cerevisiae*, *K. marxianus*, *W. anomalus*, *K. lactis* and other yeasts (28). It was shown that  
98 Eat1 is responsible for 80% and 50% of ethyl acetate production in *K. lactis* and *S.*  
99 *cerevisiae*, respectively. In this study, we show that Eat1 of *K. lactis* is located in the  
100 mitochondria. In addition, we used *in silico* analyses and fermentations of bulk ethyl acetate  
101 producing yeasts to support this view for the location of Eat1 in other yeasts as well.

102 **Results**103 *Localisation of Eat1 in yeast*

104 Huh *et al.* (2003) performed a global protein localisation study in *S. cerevisiae* (29). This  
105 included the hypothetical protein YGR015C, which was later identified as the *S. cerevisiae*  
106 homolog of Eat1 (28). The *S. cerevisiae* Eat1 was tracked to the mitochondria (29), which  
107 suggests that Eat1 may be located in the mitochondria of bulk ethyl acetate producing yeast  
108 as well. We initially tested the hypothesis by overexpressing the *W. anomalus eat1* fused  
109 with *mCherry* at the C-terminus from a multi-copy plasmid in *S. cerevisiae*. The fusion protein  
110 was generally localised to the mitochondria of *S. cerevisiae*. However, we also observed a  
111 number of artefacts associated with heterologous overexpression of fluorescent protein  
112 fusions, such as variations of the fluorescence within the cell population or protein  
113 aggregation (unpublished result). To obtain more conclusive results, we fused Eat1 with  
114 yEGFP (yeast-enhanced green fluorescent protein) at the C-terminus in *K. lactis* CBS 2359  
115  $\Delta ku80$ . *K. lactis* CBS 2359 was chosen because it was previously demonstrated that Eat1 is  
116 the main enzyme responsible for bulk ethyl acetate production in this yeast (28).

117 The location of Eat1-yEGFP in living cells of *K. lactis* CBS 2359  $\Delta ku80 eat1-yegfp$  was  
118 visualised using confocal microscopy. Eat1-yEGFP was clearly concentrated in structures  
119 within the cell (Figure 2A). The mitochondria of these cells were stained with MitoTracker  
120 Deep Red FM (Figure 2B). The overlay of the two images showed that the signals of yEGFP  
121 and the mitochondrial marker overlap almost completely (Figure 2C). However, there are  
122 some areas where Eat1 fluorescence did not overlap with MitoTracker. This may be an  
123 artefact of the dye but could also indicate that Eat1 is located in multiple organelles.  
124 Nevertheless, the *in vivo* experiments showed that Eat1 is mostly located in the mitochondria  
125 of *K. lactis* CBS 2359  $\Delta ku80$ . To exclude that the Eat1-yEGFP fusion affected the function of  
126 Eat1, we compared the ethyl acetate production of *K. lactis* CBS 2359  $\Delta ku80 eat1-yegfp$  and  
127 its parental strain. The strains were cultivated in 50 mL YM medium without iron

128 supplementation. The strain producing the Eat1-yEGFP fusion was still able to synthesise  
129 ethyl acetate (Figure 3). Surprisingly, the ethyl acetate titre achieved by *K. lactis* CBS 2359  
130  $\Delta ku80$  *eat1-yEGFP* was 3.75-fold higher compared to *K. lactis* CBS 2359  $\Delta ku80$ . The reason  
131 for this increase is not clear, but it demonstrated that the Eat1-yEGFP fusion is still  
132 functional. These results show that ethyl acetate itself is primarily a mitochondrial product of  
133 *K. lactis* CBS 2359  $\Delta ku80$ .

134 *Continuous fermentations indicate a common mechanism of ethyl acetate synthesis in yeast*

135 As Eat1 is located in the mitochondria of *S. cerevisiae* and *K. lactis* CBS 2359  $\Delta ku80$ , we  
136 were wondering whether it is located in the mitochondria of other bulk ethyl acetate  
137 producing yeasts as well. The expression of GFP-fused proteins in these yeasts is  
138 cumbersome because of their poor genetic accessibility. We attempted to transform *W.*  
139 *anomalus* DSM 6766 and *K. marxianus* DSM 5422, but were not successful. To gain further  
140 insight on the location of ethyl acetate synthesis in other yeast strains, we compared the  
141 natural producers *in vivo* instead. We reasoned that if the conditions that trigger bulk ethyl  
142 acetate formation are similar, the underlying pathways are likely shared as well, including the  
143 cellular location of Eat1. However, there are no studies that accurately compare ethyl acetate  
144 production by multiple yeasts under the same conditions. Moreover, many studies on bulk  
145 ethyl acetate synthesis in yeast often did not control or measure parameters such as oxygen  
146 levels or ethyl acetate evaporation (3). This makes metabolic comparisons between different  
147 yeast species impossible. To resolve the issue, we examined bulk ethyl acetate production in  
148 five yeast species under the same controlled conditions. We used aerobic, iron-limited  
149 chemostats to induce ethyl acetate production in *W. anomalus* DSM 6766, *C. fabianii* CBS  
150 5640, *C. jadinii* CECT 1946, *K. marxianus* DSM 5422, and *K. lactis* CBS 2359. When 1 mM  
151  $\text{FeSO}_4$  was added to the medium, all five yeasts fully consumed the glucose, and virtually no  
152 ethyl acetate or other fermentation products were formed (Figure 4). To induce ethyl acetate  
153 production, iron was omitted from the medium. Sufficient iron impurities were present to  
154 stably support between  $3.4 \pm 0.2$  and  $8.3 \pm 0.0$  g<sub>DW</sub>/L biomass (Figure 4A). Under iron-limited

155 conditions, the yeast strains consumed between  $54.5 \pm 0.0$  and  $79.3 \pm 0.0$  g/L glucose  
156 (Figure 4B). Iron limitation induced ethyl acetate production in the five yeast species (Figure  
157 4C). The amount of ethyl acetate removed through gas stripping was added to the  
158 concentrations measured in the liquid. The headspace contained  $25.9 \pm 0.0$  % of the total  
159 ethyl acetate produced. The highest ethyl acetate titres were obtained with *W. anomalus*  
160 DSM 6766 and *K. marxianus* DSM 5422 ( $11.6 \pm 0.2$  and  $10.7 \pm 0.3$  g/L, respectively).  
161 However, *K. marxianus* DSM 5422 consumed more sugar, resulting in a lower ethyl acetate  
162 yield (Figure 4D). *W. anomalus* DSM 6766 and *C. fabianii* CBS 5640 were the best ethyl  
163 acetate producers in terms of yield. They produced  $0.17 \pm 0.00$  g<sub>EA</sub>/g<sub>glucose</sub> and  $0.16 \pm 0.01$   
164 g<sub>EA</sub>/g<sub>glucose</sub>, respectively. *K. lactis* CBS 2359 produced the least ethyl acetate per glucose  
165 ( $0.04 \pm 0.01$  g<sub>EA</sub>/g<sub>glucose</sub>). The maximum theoretical pathway yield of ethyl acetate on glucose  
166 is  $0.49$  g<sub>EA</sub>/g<sub>glucose</sub>.

167 Besides ethyl acetate, the yeasts also formed significant amounts of ethanol or acetate as  
168 by-products (Figure 4E and 4F, respectively). Crabtree-negative yeasts generally do not  
169 produce ethanol under aerobic conditions like the ones used in this study. However, iron  
170 limitation results in a metabolic deregulation which leads to ethanol production (16, 20). *W.*  
171 *anomalus* DSM 6766, *C. fabianii* CBS 5640 and *C. jadinii* CECT 1946 produced between  
172  $0.02 \pm 0.01$ , and  $0.01 \pm 0.00$  g<sub>ethanol</sub>/g<sub>glucose</sub>. This was significantly lower compared to *K.*  
173 *marxianus* DSM 5422 and *K. lactis* CBS 2359, which produced  $0.11 \pm 0.01$ , and  $0.23 \pm 0.01$   
174 (Figure 4E). The yeasts also produced between  $0.02 \pm 0.00$ , and  $0.12 \pm 0.01$  g<sub>acetate</sub>/g<sub>glucose</sub>  
175 (Figure 4F).

176 The five tested yeasts produced ethyl acetate under aerobic and iron-limited conditions.  
177 However, there were significant levels of ethanol and acetate produced. These products  
178 indicate that glucose is catabolised in the cytosol as well, despite the aerobic conditions. The  
179 effect was most pronounced in *K. lactis* CBS 2359, which produced 6.1-fold more ethanol  
180 than ethyl acetate. Most of this ethyl acetate was produced by the mitochondrial Eat1 (Figure  
181 2), despite the high carbon flux in the cytosol (Figure 4EF). The remaining four yeasts

182 produced ethyl acetate under the same iron-limited conditions as *K. lactis* CBS 2359, which  
183 suggests that the ethyl acetate produced by these yeasts is of mitochondrial origin as well.

184 *In silico* indications for Eat1 localisation in yeast

185 Acetyl-CoA used for bulk ethyl acetate synthesis is produced in the mitochondria. We  
186 investigated whether the five yeast strains are able to transport acetyl-CoA from the  
187 mitochondria to the cytosol via citrate. The enzyme needed for the realisation of this pathway  
188 is the cytosolic ATP-citrate lyase (Figure 1). We used BlastP to search for homologs of three  
189 fungal ATP-citrate lyase proteins in *W. anomalus*, *C. jadinii*, *C. fabianii*, *K. marxianus* and *K.*  
190 *lactis*. The ATP-citrate lyase homologs originated from *Yarrowia lipolytica* CLIB 122,  
191 *Aspergillus nidulans* FGSC A4 and the *Rhodospiridium toruloides* IFO 0880. None of the  
192 bulk ethyl acetate producing yeasts contained apparent ATP-citrate lyase homologs. The  
193 absence of the ATP-citrate lyase suggests that ethyl acetate-producing yeasts cannot  
194 transport acetyl-CoA to the cytosol (22, 26). Bulk ethyl acetate synthesis by Eat1 is therefore  
195 more likely to be located in the mitochondria.

196 The sub-cellular location of proteins can also be predicted *in silico* based on their primary  
197 sequence. We predicted the location of nine Eat1 homologs originating from nine bulk ethyl  
198 acetate producing yeast species (28). The mitochondrial citrate synthase (Cit1) and the  
199 cytosolic Atf1 and Atf2 from *S. cerevisiae* were included in the analysis as controls. Seven  
200 tools were used in the analysis: MitoProt II (30), MultiLoc 2 (31), Yloc (32), WoLF PSORT  
201 (33), Protein Prowler (34) and BacCellLo (35) and MitoFates (36). The Eat1 homologs were  
202 generally predicted as mitochondrial (Figure 5). The Eat1 homologs of *K. lactis*, *K. marxianus*  
203 and *Wickerhamomyces ciferri* were predicted as mitochondrial by all seven tools. The least  
204 mitochondrial localisation predictions were given to the *W. anomalus* and *C. fabianii* Eat1  
205 homologs. Most of the non-mitochondrial predictions were assigned by Protein Prowler, Mito  
206 Prot II and MitoFates. These tools also did not identify the *S. cerevisiae* Eat1 protein as  
207 mitochondrial. This indicates that the predictions made by these tools may not be reliable for

208 the Eat1 homologs. On the other hand, MultiLoc2 and WoLF PSORT predicted all the  
209 proteins as mitochondrial, including the *S. cerevisiae* and *K. lactis* Eat1 homologs. These two  
210 tools also performed better compared to Protein Prowler (31, 37).

## 211 Discussion

212 In this study, we included the cellular location of Eat1 into the hypothetical model of bulk  
213 ethyl acetate production in yeast. This AAT was previously linked to 80 % and 50 % of ethyl  
214 acetate synthesis in *K. lactis* and *S. cerevisiae*, respectively (28). Results presented here  
215 showed that Eat1 is a mitochondrial protein in both yeasts. However, the current model of  
216 bulk ethyl acetate production assumes that cytosolic AATs are responsible for ethyl acetate  
217 formation (17). The mitochondrial location of Eat1 in *K. lactis* CBS 2359 described in this  
218 study disagrees with this assumption. It is also likely that bulk ethyl acetate by other yeast is  
219 of mitochondrial origin as well. Ideally, confocal microscopy could be used to confirm this.  
220 However, this is hampered by the lack of genetic tools needed to perform gene fusions in  
221 other bulk ethyl acetate producing yeast. It is also not possible to discriminate between the  
222 mitochondrial and cytosolic acetyl-CoA flux using  $^{13}\text{C}$  tracking experiments as the same  
223 carbon atoms are removed during the cleavage of pyruvate in both compartments. The  
224 acetyl-CoA produced in the mitochondria is therefore identical to the one produced in the  
225 cytosol. The *in silico* tools used in this study generally predicted that all known Eat1  
226 homologs are mitochondrial. The apparent lack of ATP-citrate lyase homologs also seems to  
227 indicate that acetyl-CoA cannot be transported to the cytosol. Mitochondrial acetyl-CoA may  
228 play a role in ethyl acetate synthesis in *S. cerevisiae* as well. This yeast contains a functional  
229 Eat1 homolog, but produces only traces of ethyl acetate (2). This is likely caused by the  
230 Crabtree-positive nature of *S. cerevisiae*. When glucose is present in excess, the main  
231 carbon flux in *S. cerevisiae* bypasses the mitochondria in favour of cytosolic ethanol  
232 formation (19, 38). It is possible that the low ethyl acetate production in *S. cerevisiae* is  
233 caused by the low mitochondrial acetyl-CoA flux.

234 *W. anomalus* DSM 6766, *C. fabianii* CBS 5640, *C. jadinii* CECT 1946, *K. marxianus* DSM  
235 5422 and *K. lactis* CBS 2359 are all Crabtree-negative yeasts. Under aerobic conditions,  
236 such yeasts convert glucose to cytosolic pyruvate and further to mitochondrial acetyl-CoA.  
237 Conditions such as iron limitation repress the synthesis of enzymes in the TCA cycle and  
238 respiratory chain (39, 40). As a consequence, ethanol is produced in the cytosol even under  
239 aerobic conditions (20, 41). In the mitochondria, iron limitation leads to the accumulation of  
240 acetyl-CoA. The accumulation may be resolved by Eat1 in the mitochondria by forming ethyl  
241 acetate (14, 18, 41). The mitochondrial localisation of Eat1 thus agrees with its proposed  
242 physiological function of preventing the accumulation of acetyl-CoA in yeast. However, more  
243 research is needed to confirm this hypothesis. It has been shown that Eat1 can function as a  
244 thioesterase *in vitro* (28). This activity could relieve acetyl-CoA accumulation by releasing  
245 acetate instead of ethyl acetate. However, it is possible that ethyl acetate formation provides  
246 ancillary benefits to the yeasts. It has been shown that ethyl acetate inhibits the growth of  
247 competitive microorganisms (42) and helps yeast disperse in the environment by attracting  
248 fruit flies (43).

249 The demonstration that Eat1 is a mitochondrial enzyme is critical for improving ethyl acetate  
250 production by microorganisms. Yeasts like *K. marxianus* and *W. anomalus* are naturally able  
251 to produce ethyl acetate at high yields. However, they also produce considerable amounts of  
252 ethanol and acetate as by-products. The acetyl-CoA and ethanol used for ethyl acetate  
253 synthesis are produced in the mitochondria and cytosol, respectively. Cytosolic pyruvate is  
254 the precursor of both substrates. Efficient ethyl acetate production would therefore require  
255 precise control over the pyruvate flux so that acetyl-CoA and ethanol production are  
256 stoichiometrically balanced. Alternatively, Eat1 can be used to produce ethyl acetate in  
257 heterologous hosts. In such cases, consideration should be given to identifying the  
258 localisation pre-sequence. In eukaryotes, N-terminal pre-sequences are cleaved from the  
259 nascent protein during translocation to the mitochondria, giving rise to the mature protein  
260 (44). Unrelated hosts may not be able to perform this cleavage. The presence of the N-

261 terminal localisation sequence has resulted in lower protein activity and stability in some  
262 cases (45, 46). Proper N-terminal processing of the Eat1 proteins may therefore improve the  
263 activity of the protein in heterologous hosts.

264 Until now it was assumed that yeasts such as *K. lactis*, *K. marxianus* and *W. anomalus*  
265 produce ethyl acetate in the cytosol. The present study has established that the synthesis  
266 occurs in mitochondria instead. This finding agrees with the proposed biological function of  
267 bulk ethyl acetate synthesis. Our understanding of ester synthesis in yeast is hereby  
268 expanded, which will enable the design of more efficient processes for the production of  
269 biobased ethyl acetate.

270

271 **Materials and Methods**272 *Strain and plasmid construction*

273 Strains and plasmids that were used in this study are listed in Table 1. Wild type yeast  
274 strains were obtained from culture collections. *Kluyveromyces lactis* CBS 2359  $\Delta ku80$  (47)  
275 was a gift from Paul Hooykaas (Leiden University). Plasmid pCY 3040-01 was a gift from  
276 Anne Robinson (Addgene plasmid # 36217). Plasmid pUG75 (48) was obtained from  
277 Euroscarf (Plasmid #P30671). *K. lactis* CBS 2359  $\Delta ku80 eat1-yEGFP$  was constructed by  
278 integrating the *yegfp* gene (49) in frame at the 3' end of *eat1*. A (GGTGGTAGTGGT)<sub>2</sub> linker  
279 was inserted between *eat1* and *yegfp*. The native *eat1* stop codon was removed. The linear  
280 integration cassette contained the linker, *yegfp* and pAgTEF1-*hphMX-tAgTEF1*, flanked by  
281 1000 bp sequence upstream and downstream of the integration site. The flanking regions,  
282 *yegfp* and pAgTEF1-*hphMX-tAgTEF1* were amplified from the *K. lactis* CBS 2359  $\Delta ku80$   
283 genome, pCY-3040-01 and pUG75, respectively. The parts were assembled to yield the  
284 plasmid pYES2-KlaEat1-yEGFP-hphMX-1000 with the HiFi assembly kit (NEB), according to  
285 manufacturer instructions. pYES2 (Invitrogen) was used as the backbone. The linear  
286 integration cassette was PCR amplified from pYES2-KlaEat1-yEGFP-hphMX-1000. 1  $\mu$ g of  
287 the cassette was transformed into *K. lactis* CBS 2359  $\Delta ku80$  with the Li-acetate method (50).  
288 Transformants were selected on plates containing 100  $\mu$ g/mL hygromycin B. Correct clones  
289 were confirmed by PCR and sequencing.

290 *Cultivation conditions*

291 Yeast and *E. coli* cultures were routinely cultivated in YPD (20 g/L glucose, 10 g/L yeast  
292 extract, 20 g/L peptone) or LB (10 g/L tryptone, 5 g/L yeast extract, 10 g/L NaCl) medium,  
293 respectively. Bacteriological agar (15 g/L) was added to make plates. Ampicillin (50  $\mu$ g/mL)  
294 and hygromycin B (100  $\mu$ g/mL) were added to the media when appropriate. Yeast and *E. coli*  
295 were grown at 30 °C and 37 °C, respectively, unless stated otherwise. All strains were stored  
296 as glycerol stocks at -80 °C. Yeast and *E. coli* strains were revived by streaking frozen

297 cultures on agar plates and cultivating until colonies appeared. Single colonies were used to  
298 inoculate liquid precultures used in further experiments.

299 The ethyl acetate production of *K. lactis* CBS 2359  $\Delta ku80$  and *K. lactis* CBS 2359  $\Delta ku80$   
300 *eat1-yEGFP* was assessed as reported previously (28). The cells were grown in 250-mL  
301 Erlenmeyer flasks containing 50 mL YM (yeast minimal) medium adapted from Thomas and  
302 Dawson, 1978 (18). YM medium contained glucose (50 g/L),  $(\text{NH}_4)_2\text{SO}_4$  (2.5 g/L),  $\text{KH}_2\text{PO}_4$   
303 (2.5 g/L), 3-(N-morpholino) propanesulfonic acid (MOPS, 23.1 g/L),  $\text{MgSO}_4$  (60 mg/L), Ca,  
304  $\text{ZnSO}_4 \cdot 7 \text{H}_2\text{O}$  (25.0 mg/L),  $\text{MnCl}_2 \cdot 4\text{H}_2\text{O}$  (4.0 mg/L),  $\text{CuSO}_4 \cdot 5 \text{H}_2\text{O}$  (2.5 mg/L),  $\text{CaCl}_2 \cdot 2 \text{H}_2\text{O}$   
305 (1.5 mg/L),  $\text{H}_3\text{BO}_3$  (1.5 mg/L)  $\text{Na}_2\text{MoO}_4 \cdot 2 \text{H}_2\text{O}$  (0.4 mg/L),  $\text{CoCl}_2$  (0.2 mg/L) and KI (0.3  
306 mg/L). The pH of the medium was set to 6.0 with 3 M NaOH. Iron was omitted from the  
307 medium. The medium was supplemented with 1 mL 1000x vitamins mix according to  
308 Verduyn *et al.* 1992 (51). The vitamins mix contained Biotin(0.05 mg/L), Ca-panthothenate (1  
309 mg/L), Nicotinic acid (1 mg/L), Inositol (25 mg/L), Thiamine-HCl (1 mg/L), Pyridoxine-  
310 HCl (1 mg/L), 4-amino benzoic acid (0.2 mg/L). Erlenmeyer flasks (neck width 34 mm) were  
311 inoculated with 0.5 mL preculture grown overnight in liquid YPD medium to an initial  $\text{OD}_{600}$  of  
312 0.03. The flasks were closed with aluminium foil and shaken at 250 rpm. Experiments were  
313 performed as biological duplicates. Ethyl acetate evaporation was not measured in shake  
314 flasks.

#### 315 *Continuous fermentations*

316 The ethyl acetate production of *W. anomalus* DSM 6766, *C. fabianii* CBS 5640, *C. jadinii*  
317 *CECT* 1946, *K. marxianus* DSM 5422, and *K. lactis* CBS 2359 was studied in aerobic  
318 continuous fermentations. The culturing was performed in 1-L DasGip bioreactors  
319 (Eppendorf). The working volume was 0.5 L. The pH was controlled at 5.0 ( $\pm$  0.05) by  
320 automatic addition of 3 M KOH. The temperature was controlled at 30°C. Cultures were kept  
321 aerobic by controlling the DO at 40%. Sufficient oxygen transfer was achieved by stirring the  
322 fermenter at 1200 rpm and automatically varying the oxygen fraction from 21% to 100%. The

323 sparging was kept constant at 6 L/h. The defined feed medium was designed to emulate the  
324 mineral composition of concentrated whey permeate augmented with ammonium sulphate  
325 (52) as closely as possible. Distilled water (dH<sub>2</sub>O) was used to prepare the medium. The  
326 medium contained (NH<sub>4</sub>)<sub>2</sub>SO<sub>4</sub> (13.16 g/L), Na<sub>2</sub>HPO<sub>4</sub>\*2 H<sub>2</sub>O (2.08 g/L), NaCl (1.39 g/L), KCl  
327 (1.89 g/L), MgSO<sub>4</sub> \*7 H<sub>2</sub>O (0.81 g/L), CaCl<sub>2</sub> \* H<sub>2</sub>O (0.139 g/L), ZnSO<sub>4</sub> \* 7 H<sub>2</sub>O (50 mg/L),  
328 CuCl<sub>2</sub> \* 2H<sub>2</sub>O (6.6 mg/L), Na<sub>2</sub>MoO<sub>4</sub> \* 2 H<sub>2</sub>O (1 mg/L), H<sub>3</sub>BO<sub>3</sub> (2 mg/L), MnSO<sub>4</sub> \* 1 H<sub>2</sub>O (1.51  
329 mg/L), CoSO<sub>4</sub> \* 7 H<sub>2</sub>O (2 mg/L), NiSO<sub>4</sub> \* 6 H<sub>2</sub>O (1 mg/L) and 4 mL/L of a 1000x vitamin mix  
330 (51). Glucose (80 g/L) was used as carbon source. 20 mL 37% HCl was added to the 20 L  
331 medium vessel to lower the pH of the medium. The dilution rate was 0.1 h<sup>-1</sup>. Ethyl acetate  
332 production was controlled by iron limitation. The producing (iron-limited) condition was  
333 achieved by omitting all sources of iron from the medium. The non-producing (iron-  
334 rich/glucose-limited) condition was achieved by adding 1 mM FeSO<sub>4</sub> to the medium vessel.  
335 Steady state was achieved after five culture volumes were exchanged during which  
336 physiological parameters remained stable. The reported numbers are an average of three  
337 sequential steady states achieved in one bioreactor. The amount of ethyl acetate in the  
338 headspace was quantified by extracting 250 µL of the bioreactor headspace through a  
339 septum with a syringe and analysing the ethyl acetate content immediately by gas  
340 chromatography (GC). The concentration of ethyl acetate in the headspace was used to  
341 calculate the mass flow of ethyl acetate continuously discharged from the fermenters. The  
342 mass flow of ethyl acetate was related to the liquid flow of 0.05 L/h and added to the ethyl  
343 acetate concentration in the liquid phase. Dry cell weight was determined in 50 mL  
344 fermentation broth.

#### 345 *Confocal microscopy*

346 Confocal microscopy was carried out on a LeicaTCS SP8 X system equipped with a 63x/1.20  
347 numeric aperture water-immersion objective. Excitation of EGFP and MitoTracker Deep Red  
348 FM (Thermo Scientific) was performed using a white light laser selecting the lasers lines 488  
349 nm and 633 nm, respectively. Confocal imaging was executed using internal filter-free

350 spectral Hybrid detectors. For EGFP detection, a spectral window of 495 to 545 nm was  
351 selected, whereas MitoTracker Deep Red FM was detected using 640 to 670 nm. Images  
352 with 1024x1024 pixels were acquired using the HyVolution software interface of Leica  
353 operating in a sequential imaging configuration. The HyVolution software includes  
354 deconvolution of the confocal images by Huygens deconvolution software (53).

### 355 *Bioinformatics*

356 The subcellular locations of proteins was predicted with six tools: MitoProt II (30), MultiLoc 2  
357 (31), Yloc (32), WoLF PSORT (33), Protein Prowler (34) and BacCelLo (35). Where  
358 applicable, the prediction settings were set to fungal. MitoFates (36) was used to predict  
359 mitochondrial pre-sequences under fungal prediction settings. BlastP under default settings  
360 was used to look for homologs of ATP citrate lyase in *C. fabianii* CBS 5640, *C. jadinii* CECT  
361 1946, *K. marxianus* DSM 5422, *W. anomalus* DSM 6766 and *K. lactis* CBS 2359. The ATP-  
362 citrate lyase from *Yarrowia lipolytica* CLIB122 (XP\_503231.1), the ATP citrate lyase subunit  
363 1 (XP\_660040.1) from *Aspergillus nidulans* FGSC A4 and the ATP-citrate synthase from  
364 *Rhodospiridium toruloides* IFO 0880 (PRQ71611.1) were used as query (54–56).

### 365 *Analytical*

366 Glucose and organic acids were analyzed by HPLC on a Thermo Scientific ICS5000 HPLC  
367 system, equipped with a Dionex DP pump, Dionex AS-AP autosampler, Dionex VWD UV  
368 detector operated at 210 nm and a Shodex RI detector operated at 35 °C. An Aminex HPX-  
369 87H cation-exchange column (Bio-Rad) was used with a mobile phase of 0.008 M H<sub>2</sub>SO<sub>4</sub> and  
370 was operated at 0.8 mL/min and 60 °C. 10 mM dimethylsulfoxide or 125 mM propionic acid  
371 were used as internal standard.

372 Volatile compounds were analysed on two gas chromatography systems equipped with a  
373 flame ionization detector (GC-FID). In both cases, 0.5 µL of liquid or 250 µL headspace  
374 sample were analysed. For liquid samples, 2 mM 1-butanol was used as internal standard.  
375 The first system used a Shimadzu 2010 gas chromatograph equipped with a 20i-s  
376 autosampler. Samples were analysed on a Stabilwax column (30 m x 0.53 mm, 0.5 µm

377 coating, Restek). The column temperature was held at 60 °C for 1 minute and increased to  
378 120 °C at a rate of 20 °C/minute. The split ratio was 20. The second system used an Agilent  
379 7890B gas chromatograph equipped with an Agilent 7693 autosampler. The compounds  
380 were separated on a Nukol™ column (30 m x 0.53 mm, 1.0 µm coating, Supelco). The  
381 column temperature was maintained at 50 °C for 2 minutes and increased to 200°C at a rate  
382 of 50 °C/minute. The split ratio was 10.

383 Dry cell weight in continuous fermentations was measured by centrifuging 50 mL culture for 5  
384 min at 4000 *x g*. The pellet was then washed with 50 mL ultrapure MilliQ water (MQ),  
385 resuspended in 3 mL MQ and dried overnight at 120 °C in a pre-weighted aluminum tray  
386 before weighing.

387

388

389 **References**

- 390 1. Park YC, Shaffer CEH, Bennett GN. 2009. Microbial formation of esters. Appl  
391 Microbiol Biotechnol 85:13–25.
- 392 2. Saerens SMG, Delvaux FR, Verstrepen KJ, Thevelein JM. 2010. Production and  
393 biological function of volatile esters in *Saccharomyces cerevisiae*. Microb Biotechnol  
394 3:165–177.
- 395 3. Löser, Urit, Bley. 2014. Perspectives for the biotechnological production of ethyl  
396 acetate by yeasts. Appl Microbiol Biotechnol 98:5397–5415.
- 397 4. Löser C, Urit T, Stukert A, Bley T. 2013. Formation of ethyl acetate from whey by  
398 *Kluyveromyces marxianus* on a pilot scale. J Biotechnol 163:17–23.
- 399 5. Passoth V, Olstorpe M, Schnurer J. 2011. Past, present and future research directions  
400 with *Pichia anomala*. Antonie Van Leeuwenhoek Int J Gen Mol Microbiol 99:121–125.
- 401 6. Fredlund E, Beerlage C, Melin P, Schnürer J, Passoth V. 2006. Oxygen and carbon  
402 source-regulated expression of PDC and ADH genes in the respiratory yeast *Pichia*  
403 *anomala*. Yeast 23:1137–1149.
- 404 7. Meersman E, Steensels J, Struyf N, Paulus T, Saels V, Mathawan M, Allegaert L,  
405 Vrancken G, Verstrepen KJ. 2016. Tuning Chocolate Flavor through Development of  
406 Thermotolerant *Saccharomyces cerevisiae* Starter Cultures with Increased Acetate  
407 Ester Production. Appl Environ Microbiol 82:732–746.
- 408 8. Löser C, Urit T, Nehl F, Bley T. 2011. Screening of *Kluyveromyces* strains for the  
409 production of ethyl acetate: Design and evaluation of a cultivation system. Eng Life Sci  
410 11:369–381.
- 411 9. Minetoki T, Bogaki T, Iwamatsu A, Fujii T, Hamachi M. 1993. The Purification,  
412 Properties and Internal Peptide Sequences of Alcohol Acetyltransferase Isolated from

- 413 *Saccharomyces cerevisiae* Kyokai No. 7. *Biosci Biotechnol Biochem* 57:2094–2098.
- 414 10. Yoshimoto H, Fujiwara D, Momma T, Tanaka K, Sone H, Nagasawa N, Tamai Y.  
415 1999. Isolation and characterization of the ATF2 gene encoding alcohol  
416 acetyltransferase II in the bottom fermenting yeast *Saccharomyces pastorianus*. *Yeast*  
417 15:409–417.
- 418 11. Verstrepen KJ, Van Laere SDM, Vanderhaegen BMP, Derdelinckx G, Dufour J-PP,  
419 Pretorius IS, Winderickx J, Thevelein JM, Delvaux FR. 2003. Expression levels of the  
420 yeast alcohol acetyltransferase genes ATF1, Lg-ATF1, and ATF2 control the formation  
421 of a broad range of volatile esters. *Appl Env Microbiol* 69:5228–5237.
- 422 12. Schneider J, Rupp O, Trost E, Jaenicke S, Passoth V, Goesmann A, Tauch A,  
423 Brinkrolf K. 2012. Genome sequence of *Wickerhamomyces anomalus* DSM 6766  
424 reveals genetic basis of biotechnologically important antimicrobial activities. *FEMS*  
425 *Yeast Res* 12:382–386.
- 426 13. Van Laere SDM, Saerens SMG, Verstrepen KJ, Van Dijck P, Thevelein JM, Delvaux  
427 FR. 2008. Flavour formation in fungi: characterisation of KIAf, the *Kluyveromyces*  
428 *lactis* orthologue of the *Saccharomyces cerevisiae* alcohol acetyltransferases Atf1 and  
429 Atf2. *Appl Microbiol Biotechnol* 78:783–792.
- 430 14. Armstrong DW, Yamazaki H. 1984. Effect of iron and EDTA on ethyl acetate  
431 accumulation in *Candida utilis*. *Biotechnol Lett* 6:819–824.
- 432 15. Fredlund E, Blank LM, Schnürer J, Schnu J, Sauer U. 2004. Oxygen- and Glucose-  
433 Dependent Regulation of Central Carbon Metabolism in *Pichia anomala*. *Appl Env*  
434 *Microbiol* 70:5905–5911.
- 435 16. Urit T, Stukert A, Bley T, Löser C. 2012. Formation of ethyl acetate by *Kluyveromyces*  
436 *marxianus* on whey during aerobic batch cultivation at specific trace element limitation.  
437 *Appl Microbiol Biotechnol* 96:1313–1323.

- 438 17. Löser C, Urit T, Keil P, Bley T. 2015. Studies on the mechanism of synthesis of ethyl  
439 acetate in *Kluyveromyces marxianus* DSM 5422. *Appl Microbiol Biotechnol* 99:1131–  
440 1144.
- 441 18. Thomas KC, Dawson PSS. 1978. Relationship between iron-limited growth and  
442 energy limitation during phased cultivation of *Candida utilis*. *Can J Microbiol* 24:440–  
443 447.
- 444 19. Pfeiffer T, Morley A. 2014. An evolutionary perspective on the Crabtree effect. *Front*  
445 *Mol Biosci* 1.
- 446 20. van Dijken JP, Weusthuis RA, Pronk JT. 1993. Kinetics of growth and sugar  
447 consumption in yeasts. *Antonie Van Leeuwenhoek* 63:343–352.
- 448 21. Van den Berg MA, Steensma HY. 1995. ACS2, a *Saccharomyces cerevisiae* gene  
449 encoding acetyl-coenzyme A synthetase, essential for growth on glucose. *Eur J*  
450 *Biochem* 231:704–713.
- 451 22. van Rossum HM, Kozak BU, Pronk JT, van Maris AJA. 2016. Engineering cytosolic  
452 acetyl-coenzyme A supply in *Saccharomyces cerevisiae*: Pathway stoichiometry, free-  
453 energy conservation and redox-cofactor balancing. *Metab Eng* 36:99–115.
- 454 23. Verstrepen KJ, Van Laere SDM, Vercammen J, Derdelinckx G, Dufour JP, Pretorius  
455 IS, Winderickx J, Thevelein JM, Delvaux FR. 2004. The *Saccharomyces cerevisiae*  
456 alcohol acetyl transferase Atf1p is localized in lipid particles. *Yeast* 21:367–376.
- 457 24. Lin JL, Wheeldon I. 2014. Dual N- and C-terminal helices are required for endoplasmic  
458 reticulum and lipid droplet association of alcohol acetyltransferases in *Saccharomyces*  
459 *cerevisiae*. *PLoS One* 9.
- 460 25. Zhu J, Lin J-L, Palomec L, Wheeldon I. 2015. Microbial host selection affects  
461 intracellular localization and activity of alcohol-O-acetyltransferase. *Microb Cell Fact*  
462 14:35.

- 463 26. Boulton CA, Ratledge C. 1981. Correlation of Lipid Accumulation in Yeasts with  
464 Possession of ATP:Citrate Lyase. *J Gen Microbiol* 127:169–176.
- 465 27. Shashi K, Bachhawat AK, Joseph R. 1990. ATP:citrate lyase of *Rhodotorula gracilis*:  
466 purification and properties. *Biochim Biophys Acta* 1033:23–30.
- 467 28. Kruis AJ, Levisson M, Mars AE, van der Ploeg M, Garcés Daza F, Ellena V, Kengen  
468 SWM, van der Oost J, Weusthuis RA. 2017. Ethyl acetate production by the elusive  
469 alcohol acetyltransferase from yeast. *Metab Eng* 41:92–101.
- 470 29. Huh W-K, Falvo J V., Gerke LC, Carroll AS, Howson RW, Weissman JS, O’Shea EK.  
471 2003. Global analysis of protein localization in budding yeast. *Nature* 425:686–691.
- 472 30. Claros MG, Vincens P. 1996. Computational method to predict mitochondrially  
473 imported proteins and their targeting sequences. *Eur J Biochem* 241:779–786.
- 474 31. Blum T, Briesemeister S, Kohlbacher O. 2009. MultiLoc2: Integrating phylogeny and  
475 Gene Ontology terms improves subcellular protein localization prediction. *BMC*  
476 *Bioinformatics* 10:274.
- 477 32. Briesemeister S, Rahnenführer J, Kohlbacher O. 2010. YLoc-an interpretable web  
478 server for predicting subcellular localization. *Nucleic Acids Res* 38:W497–W502.
- 479 33. Horton P, Park K-J, Obayashi T, Fujita N, Harada H, Adams-Collier CJ, Nakai K. 2007.  
480 WoLF PSORT: protein localization predictor. *Nucleic Acids Res* 35:W585–W587.
- 481 34. Boden M, Hawkins J. 2005. Prediction of subcellular localization using sequence-  
482 biased recurrent networks. *Bioinformatics* 21:2279–2286.
- 483 35. Pierleoni A, Martelli PL, Fariselli P, Casadio R. 2006. BaCellLo: a balanced subcellular  
484 localization predictor. *Bioinformatics* 22:e408–e416.
- 485 36. Fukasawa Y, Tsuji J, Fu S-C, Tomii K, Horton P, Imai K. 2015. MitoFates: improved  
486 prediction of mitochondrial targeting sequences and their cleavage sites. *Mol Cell*

- 487 Proteomics 14:1113–1126.
- 488 37. Casadio R, Martelli PL, Pierleoni A. 2008. The prediction of protein subcellular  
489 localization from sequence: a shortcut to functional genome annotation. Briefings  
490 Funct Genomics Proteomics 7:63–73.
- 491 38. De Deken RH. 1966. The Crabtree Effect: A Regulatory System in Yeast. J Gen  
492 Microbiol 44:149–156.
- 493 39. Puig S, Askeland E, Thiele DJ. 2005. Coordinated Remodeling of Cellular Metabolism  
494 during Iron Deficiency through Targeted mRNA Degradation. Cell 120:99–110.
- 495 40. Shakoury-Elizeh M, Tiedeman J, Rashford J, Ferea T, Demeter J, Garcia E, Rolfes R,  
496 Brown PO, Botstein D, Philpott CC. 2004. Transcriptional remodeling in response to  
497 iron deprivation in *Saccharomyces cerevisiae*. Mol Biol Cell 15:1233–43.
- 498 41. Löser C, Urit T, Forster S, Stukert A, Bley T. 2012. Formation of ethyl acetate by  
499 *Kluyveromyces marxianus* on whey during aerobic batch and chemostat cultivation at  
500 iron limitation. Appl Microbiol Biotechnol 96:685–696.
- 501 42. Fredlund E, Druvefors UA, Olstorpe MN, Passoth V, Schnurer J. 2004. Influence of  
502 ethyl acetate production and ploidy on the anti-mould activity of *Pichia anomala*.  
503 FEMS Microbiol Lett 238:133–137.
- 504 43. Christiaens JFF, Franco LMM, Cools TLL, De Meester L, Michiels J, Wenseleers T,  
505 Hassan BAA, Yaksi E, Verstrepen KJJ, De Meester L, Michiels J, Wenseleers T,  
506 Hassan BAA, Yaksi E, Verstrepen KJJ. 2014. The Fungal Aroma Gene *ATF1*  
507 Promotes Dispersal of Yeast Cells through Insect Vectors. Cell Rep 9:425–432.
- 508 44. Wiedemann N, Pfanner N, Ryan MT. 2001. The three modules of ADP/ATP carrier  
509 cooperate in receptor recruitment and translocation into mitochondria. EMBO J  
510 20:951–960.

- 511 45. Veling MT, Reidenbach AG, Freiberger EC, Kwiecien NW, Hutchins PD, Drahnak MJ,  
512 Jochem A, Ulbrich A, Rush MJP, Russell JD, Coon JJ, Pagliarini DJ. 2017. Multi-omic  
513 Mitoprotease Profiling Defines a Role for Oct1p in Coenzyme Q Production. *Mol Cell*  
514 68:970–977.
- 515 46. Vögtle F-N, Prinz C, Kellermann J, Lottspeich F, Pfanner N, Meisinger C. 2011.  
516 Mitochondrial protein turnover: role of the precursor intermediate peptidase Oct1 in  
517 protein stabilization. *Mol Biol Cell* 22:2135–2143.
- 518 47. Kooistra R, Hooykaas PJJ, Steensma HY. 2004. Efficient gene targeting in  
519 *Kluyveromyces lactis*. *Yeast* 21:781–792.
- 520 48. Hegemann JH, Heick SB. 2011. Delete and repeat: A comprehensive toolkit for  
521 sequential gene knockout in the budding yeast *Saccharomyces cerevisiae*. *Methods*  
522 *Mol Biol* 765:189–206.
- 523 49. Young CL, Raden DL, Caplan JL, Czymmek KJ, Robinson AS. 2012. Cassette series  
524 designed for live-cell imaging of proteins and high-resolution techniques in yeast.  
525 *Yeast* 29:119–136.
- 526 50. Gietz DR, Woods RA. 2002. Transformation of yeast by lithium acetate/single-  
527 stranded carrier DNA/polyethylene glycol method. *Methods Enzymol* 350:87–96.
- 528 51. Verduyn C, Postma E, Scheffers WA, Van Dijken JP. 1992. Effect of benzoic acid on  
529 metabolic fluxes in yeasts: A continuous culture study on the regulation of respiration  
530 and alcoholic fermentation. *Yeast* 8:501–517.
- 531 52. Urit T, Löser C, Wunderlich M, Bley T. 2011. Formation of ethyl acetate by  
532 *Kluyveromyces marxianus* on whey: studies of the ester stripping. *Bioprocess Biosyst*  
533 *Eng* 34:547–559.
- 534 53. Borlinghaus RT, Kappel C. 2016. HyVolution—the smart path to confocal super-  
535 resolution. *Nat Methods* 13:i–iii.

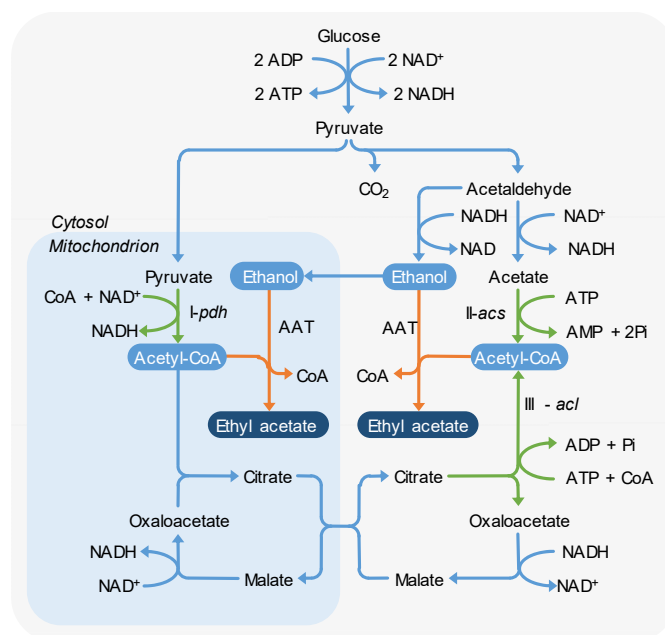
- 536 54. Galagan JE, Calvo SE, Cuomo C, Ma LJ, Wortman JR, Batzoglu S, Lee SI,  
537 Baştürkmen M, Spevak CC, Clutterbuck J, Kapitonov V, Jurka J, Scazzocchio C,  
538 Farman M, Butler J, Purcell S, Harris S, Braus GH, Draht O, Busch S, D'Enfert C,  
539 Bouchier C, Goldman GH, Bell-Pedersen D, Griffiths-Jones S, Doonan JH, Yu J,  
540 Vienken K, Pain A, Freitag M, Selker EU, Archer DB, Peñalva MÁ, Oakley BR,  
541 Momany M, Tanaka T, Kumagai T, Asai K, Machida M, Nierman WC, Denning DW,  
542 Caddick M, Hynes M, Paoletti M, Fischer R, Miller B, Dyer P, Sachs MS, Osmani SA,  
543 Birren BW. 2005. Sequencing of *Aspergillus nidulans* and comparative analysis with *A.*  
544 *fumigatus* and *A. oryzae*. *Nature* 438:1105–1115.
- 545 55. Dujon B, Sherman D, Fischer G, Durrens P, Casaregola S, Lafontaine I, de Montigny  
546 J, Marck C, Neuvéglise C, Talla E, Goffard N, Frangeul L, Aigle M, Anthouard V,  
547 Babour A, Barbe V, Barnay S, Blanchin S, Beckerich J-M, Beyne E, Bleykasten C,  
548 Boisramé A, Boyer J, Cattolico L, Confanioleri F, de Daruvar A, Despons L, Fabre E,  
549 Fairhead C, Ferry-Dumazet H, Groppi A, Hantraye F, Hennequin C, Jauniaux N, Joyet  
550 P, Kachouri R, Kerrest A, Koszul R, Lemaire M, Lesur I, Ma L, Muller H, Nicaud J-M,  
551 Nikolski M, Oztas S, Ozier-Kalogeropoulos O, Pellenz S, Potier S, Richard G-F,  
552 Straub M-L, Suleau A, Swennen D, Tekaiia F, Wésolowski-Louvel M, Westhof E, Wirth  
553 B, Zeniou-Meyer M, Zivanovic I, Bolotin-Fukuhara M, Thierry A, Bouchier C, Caudron  
554 B, Scarpelli C, Gaillardin C, Weissenbach J, Wincker P, Souciet J-L. 2004. Genome  
555 evolution in yeasts. *Nature* 430:35–44.
- 556 56. Coradetti ST, Pinel D, Geiselman G, Ito M, Mondo S, Reilly MC, Cheng Y-F, Bauer S,  
557 Grigoriev I, Gladden JM, Simmons BA, Brem R, Arkin AP, Skerker JM. 2018.  
558 Functional genomics of lipid metabolism in the oleaginous yeast *Rhodospiridium*  
559 *toruloides*. *Elife* 7.
- 560
- 561

562 **Acknowledgements**

563 We would like to acknowledge the BE-Basic foundation and AkzoNobel Specialty Chemicals

564 for funding the research.

565

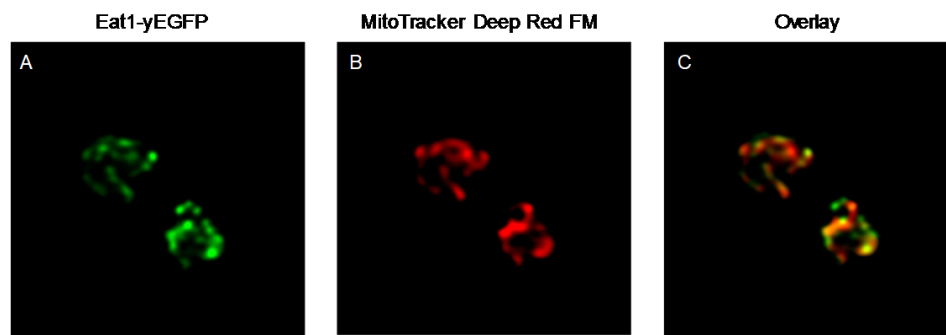


566

567 Figure 1: Potential pathways of ethyl acetate production via an AAT in yeast. The AAT  
 568 catalysed reaction is indicated in orange. The three reactions forming acetyl-CoA during  
 569 glucose catabolism are shown in green. Reaction I: pyruvate dehydrogenase (*pdh*), Reaction  
 570 II: acetyl-CoA synthetase (*acs*), Reaction III: ATP-citrate lyase (*acl*).

571

572



573

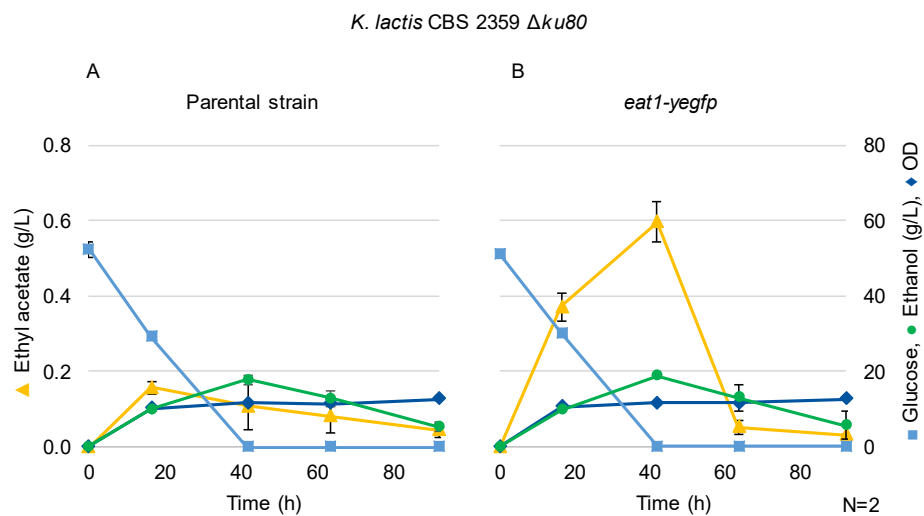
574 Figure 2. Visualisation of Eat1 in the mitochondria of *K. lactis* CBS 2359  $\Delta ku80$  *eat1-yegfp*.

575 (A) Visualisation of Eat1-yEGFP. (B) Mitochondria visualised by MitoTracker Deep Red FM.

576 (C) Overlay of the two signals. The images shown are representative of the entire cell

577 population.

578

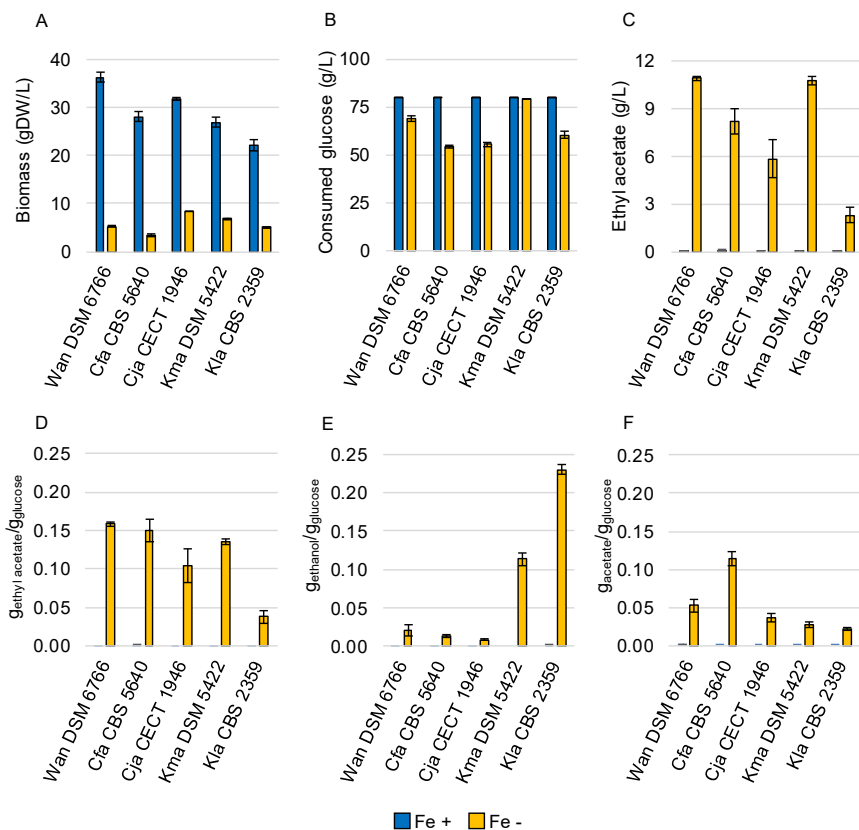


579

580 Figure 3. Fermentation profiles of (A) *K. lactis* CBS 2359  $\Delta ku80$  and (B) *K. lactis* CBS 2359  
581  $\Delta ku80$  *eat1-yEGFP* growing in shake flasks in 50 ml YM medium without iron  
582 supplementation. The numbers shown are the averages of biological duplicates. Error bars  
583 represent the standard deviation. Ethyl acetate evaporation was not measured.

584

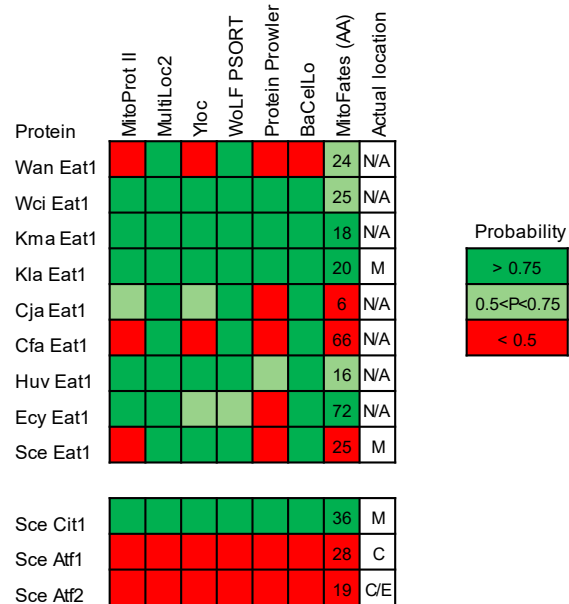
585



586  
 587 Figure 4. Cultivation parameters of five different yeast species that were grown in aerobic,  
 588 pH-controlled chemostats in the presence or absence of 1 mM of FeSO<sub>4</sub>. The numbers  
 589 shown are averages of three steady states. Error bars indicate standard deviation. The  
 590 amount of ethyl acetate that was removed by gas stripping was determined by headspace  
 591 measurements and was added to the amount that was measured in the liquid phase. (A)  
 592 Biomass concentration. (B) Glucose consumption. (C) Ethyl acetate titre. (D, E, F) The yields  
 593 of ethyl acetate, ethanol and acetate on glucose consumed, respectively.

594

595



596

597 Figure 5. Predicted probabilities of mitochondrial localisation of the Eat1 proteins. Seven  
 598 tools were used to predict the mitochondrial localisation of nine Eat1 homologs from 9 yeast  
 599 species. The numbers in the column represent the length of the pre-sequence, predicted by  
 600 MitoFates. Abbreviations: Wan - *Wickerhamomyces anomalus*, Wci - *Wickerhamomyces*  
 601 *ciferrii*, Kma – *Kluyveromyces marxianus*, Kla – *Kluyveromyces lactis*, Cja – *Cyberlindnera*  
 602 *jadinii*, Cfa – *Cyberlindnera fabianii*, Huv – *Hanseniaspora uvarum*, Ecy – *Eremothecium*  
 603 *cymbalarie*, ScE – *Saccharomyces cerevisiae*, M – mitochondria, C – cytosol, E –  
 604 endoplasmic reticulum, N/A – not available

605

606 Table 1: Strains and plasmids used and created during this study.

Strain	Characteristics	Source
<i>Cyberlindnera fabianii</i> CBS 5640	Wild type strain	CBS
<i>Cyberlindnera jadinii</i> CECT 1946	Wild type strain	CECT
<i>Kluyveromyces marxianus</i> DSM 5422	Wild type strain	DSMZ
<i>Wickerhamomyces anomalus</i> DSM 6766	Wild type strain	DSMZ
<i>Kluyveromyces lactis</i> CBS 2359	Wild type strain	CBS
<i>Kluyveromyces lactis</i> CBS 2359 <i>Δku80</i>	Disruption of KU80	(47)
<i>Kluyveromyces lactis</i> CBS 2359 <i>Δku80 eat1-yegfp</i>	Disruption of KU80, Eat1 labelled with a C-terminal yEGFP	This study
<i>E. coli</i> NEB5α	Cloning strain	New England Biolabs
<b>Plasmids</b>		
pUG75	HygR marker template	(48)
pCY-3040-01	yEGFP template	(49)
pYES2		Invitrogen
pYES2-KlaEat1-yEGFP-hphMX-1000	Plasmid carrying the <i>yegfp</i> integration cassette targeting the 3' end of the <i>K. lactis eat1</i> locus with 1000 bp homologous regions	This study

607